DC Microgrids—Part I: A Review of Control Strategies and Stabilization Techniques

Tomislav Dragičević, *Member, IEEE*, Xiaonan Lu, *Member, IEEE*, Juan C. Vasquez, *Senior Member, IEEE*, and Josep M. Guerrero, *Fellow, IEEE*

***Abstract*—This paper presents a review of control strategies, stability analysis, and stabilization techniques for dc microgrids (MGs). Overall control is systematically classified into local and coordinated control levels according to respective functionalities in each level. As opposed to local control, which relies only on local measurements, some line of communication between units needs to be made available in order to achieve the coordinated control. Depending on the communication method, three basic coordinated control strategies can be distinguished, i.e., decentralized, centralized, and distributed control. Decentralized control can be regarded as an extension of the local control since it is also based exclusively on local measurements. In contrast, centralized and distributed control strategies rely on digital communication technologies. A number of approaches using these three coordinated control strategies to achieve various control objectives are reviewed in this paper. Moreover, properties of dc MG dynamics and stability are discussed. This paper illustrates that tightly regulated point-of-load converters tend to reduce the stability margins of the system since they introduce negative impedances, which can potentially oscillate with lightly damped power supply input filters. It is also demonstrated that how the stability of the whole system is defined by the relationship of the source and load impedances, referred to as the minor loop gain. Several prominent specifications for the minor loop gain are reviewed. Finally, a number of active stabilization techniques are presented.**

***Index Terms*—Coordinated control, DC microgrid (MG), impedance specifications, local control, stability.**

Nomenclature

AVP	Adaptive voltage positioning.
BLDC	Brushless dc.
CC	Central controller.
CPL	Constant power load.
DBS	DC bus signaling.
DCL	Digital communication link.
DG	Distributed generator.
DPS	Distributed power system.
EET	Extra element theorem.
ESAC	Energy-storage analysis consortium.
ESS	Energy-storage system.
EV	Electric vehicle.
GM	Gain margin.
GMPM	Gain margin and phase margin.
LC	Local controller.
MG	Microgrid.
MPPT	Maximum power point tracking.
OA	Opposing argument.
PCC	Point of common coupling.
PD	Proportional derivative.
PI	Proportional integral.
PLC	Power line communication.
PLS	Power line signaling.
PM	Phase margin.
POL	Point of load.
PR	Proportional resonant.
PV	Photovoltaics.
RES	Renewable energy source.
RHP	Right-half plane.
TF	Transfer function.
VR	Virtual resistance.
$b_{\rm i}(t)$	Input bias of node #*i*.
C	POL converter filter capacitor.
D	POL converter steady-state duty cycle.
$G_c(s)$	TF of the voltage controller.
$G_{\rm vd}(s)$	TF describing the relation between converter duty ratio and output voltage.
$G_{\rm vg}(s)$	TF describing the relation between line disturbance and output voltage.
$G_{\rm vd,filt}(s)$	TF describing the relation between converter duty ratio and output voltage after the application of input filter.
$H(s)$	Voltage sensor gain.
$i_{\rm POL}$	Input current of the POL converter.
$i_{\rm load}$	Output current of the POL converter.
L	POL converter inductance.
m_p, m_c	Droop coefficients with power or current feedback.
N_i	Set of nodes adjacent to node #*i*.
$P_{\rm oi}$	Output power of converter #*i*.
$i_{\rm oi}$	Output current of converter #*i*.
P	DC load power.
$P_{{\rm load}i}$	Output power of POL converter #*i*.
$P_{\rm source}$	Source power.
R	Load resistance.
$R_{\rm inc}$	POL converter incremental resistance.
R_L	Series resistance of the filter inductor.
SoC	State of charge.
s	Laplace operator.
$T(s)$	Loop gain of the POL converter control loop.

Manuscript received March 27, 2015; revised July 19, 2015; accepted September 7, 2015. Date of publication September 15, 2015; date of current version January 28, 2016. Recommended for publication by Associate Editor T.-F. Wu.

T. Dragičević, J. C. Vasquez, and J. M. Guerrero are with the Department of Energy Technology, Aalborg University, Aalborg 9100, Denmark (e-mail: tdr@et.aau.dk; juq@et.aau.dk; joz@et.aau.dk).

X. Lu is with the Energy Systems Division, Argonne National Laboratory, Lemont, IL 60439 USA (e-mail: xlu@anl.gov).

Color versions of one or more of the figures in this paper are available online at http://ieeexplore.ieee.org.

Digital Object Identifier 10.1109/TPEL.2015.2478859

$T_{\text{MLG}}(s)$	Minor loop gain.
$v^*_{\text{DC}i}$	DC-link voltage reference value of converter #i.
v^*_{DC}	Nominal dc-link voltage.
v_{DC}	DC-link voltage.
v_{ref}	Reference value of the load voltage.
v_s	DC source voltage.
v_{load}	Load voltage.
$1/V_m$	PWM gain.
$x_i(t)$	Variable of interest in node #*i* used in the consensus algorithm.
$Z_N(s)$	Input impedance of the POL converter if control loop operates ideally (closed-loop input impedance in a low-frequency region).
$Z_D(s)$	Input impedance of the POL converter without control loop (open-loop input impedance).
$Z_{\text{in}}(s)$	Closed-loop input impedance of the POL converter in the whole frequency region.
$Z_{\text{out}}(s)$	Open-loop output impedance of the POL converter.
$Z_s(s)$	Output impedance of the source.
Θ	Graph Laplacian of the communication network.
θ_{ij}	Elements of Θ.

I. Introduction

ENVIRONMENTAL concerns and reduction of fossil fuel reserves gave rise to a growing increase in the penetration of distributed generators (DGs) that include renewable energy sources (RESes), energy storage systems (ESSes), and new types of loads like electric vehicles (EVs) and heat pumps in the modern power systems. However, these new components may pose many technical and operational challenges should they continue to be integrated in an uncoordinated way, as is the case today. Appearing in large numbers and scattered across the large geographical areas of interconnected networks, some of the most prominent problems that they can introduce in the system's operating conditions include deteriorated voltage profile, congestions in transmission lines, and reduction of frequency reserves [1].

The idea of merging small variable nature sources with ESSes and controllable loads into flexible entities that are called microgrids (MGs) has been presented more than a decade ago [2], as a possible solution to achieve more traceable control from the system point of view. MGs can operate autonomously or be grid-connected, and depending on the type of voltage in the point of common coupling (PCC), ac, and dc MGs can be distinguished [3]. While remarkable progress has been made in improving the performance of ac MGs during the past decade [4]–[11], dc MGs have been recognized as more attractive for numerous uses due to higher efficiency, more natural interface to many types of RES and ESS, better compliance with consumer electronics, etc. [12]. Besides, when components are coupled around a dc bus, there are no issues with reactive power flow, power quality, and frequency regulation, resulting in a notably less complex control system [13]–[18].

DGs are connected to a dc MG almost exclusively through a controllable power electronic interface converters and regulation of the common dc bus voltage is the main control priority. Droop control is a popular method of achieving this by means of cooperative operation among paralleled converters without digital communication links (DCL) [17], [19]. The method is based on adding a so-called virtual resistance (VR) control loop on top of the converter's voltage regulator which allows current sharing, while providing active damping to the system and plug and play capability at the same time [20], [21].

However, in spite of these attractive features, there are several drawbacks that limit the applicability of droop in its basic shape. The most important ones are load-dependent voltage deviation and the fact that the propagation of voltage error along resistive transmission lines causes deterioration of current sharing. A secondary controller needs to be implemented in order to restore the voltage and tertiary controller so as to ensure precise current flow among different buses [12]. There are several options on how to implement this controller. As for that, while the conventional approach uses a centralized controller which collects information from all units via low-bandwidth DCLs [3], a very active field of research is focused on resolution of these problems via distributed control[1] [22], [23]. As a way to realize various distributed control strategies, the application of consensus algorithms in dc MGs has recently emerged as a popular and fashionable approach [22], [24], [25].

Another problem with the basic droop method is its inability to achieve coordinated performance of multiple components with different characteristics (i.e., ESSes, RESes, utility mains, controllable loads, etc.). In that case, either a decentralized, centralized, or distributed supervisory control needs to be implemented on top of it to decide whether the unit should operate in droop or some other specific control mode, such as maximum power point tracking (MPPT) [26], [27], or regulated charging mode [28]. Except for setting operating modes and managing secondary/tertiary control, communication technology can also be used to realize advanced functions, such as unit commitment, optimization procedures, or manipulation of internal *I–V* characteristics by imposing adaptive mechanisms [14], [28]–[30].

Along with precise voltage and current regulation, as well as system level coordination, stable operation of the MG needs to be ensured in all operating conditions. Tightly regulated point of load (POL) converters present a challenge from that point of view since they introduce a negative impedance characteristic within the bandwidth of their control loops [31], [32]. This peculiar feature reduces the effective damping and can even cause instability of the entire system. The relationship between source and load impedances, often referred to as the minor loop gain, is an important quantity which can be used for determining stability [31]. Different specifications for the minor loop gain have been proposed not only to ensure stability but also to maintain good system dynamics after connecting additional elements such as input filters [31], [33]–[39]. Modeling of the entire state space is an alternative option which explicitly takes into account the complete system but does not provide such a good insight into dynamics as the impedance-based approach. A

[1]The term "distributed control" refers to the situation where information is exchanged through DCLs only between units, rather than between units and a central aggregator.

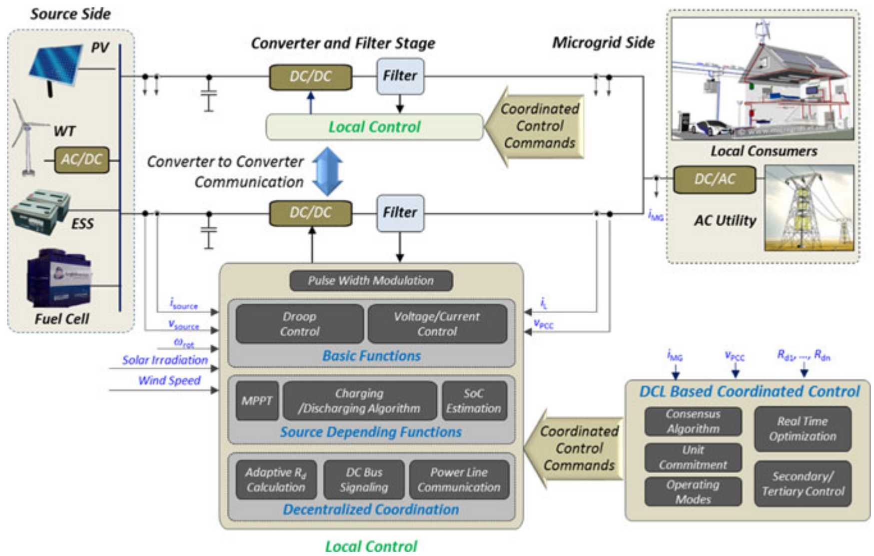

Fig. 1. Systematic control diagram in dc MGs.

variety of passive and active stabilization techniques have been developed using both methods in order to improve the damping of the system [40]–[44].

The aim of this paper is to provide an overview of control strategies, stability analysis tools, and stabilization techniques used in dc MGs. It is organized as follows. In Section II, basic control principles are presented. It is demonstrated how the overall converter control can be split into local and coordinated controls. Section III explores in more depth a number of functionalities within the local control, while coordinated control is addressed in Section IV. A detailed analysis of the stability problem is presented in Section V, where it is shown how a dynamic model of the whole dc MG system can be conveniently divided into a source and load subsystems which are characterized by their respective impedances. It is explained how the relationship of these impedances defines the stability of the system, and several prominent impedance specifications and stabilization principles are reviewed. Concluding remarks and an overview of future research trends can be found in Section VI.

II. DC MG Control Principles

In order to guarantee stable and efficient operation of a dc MG, effective control strategies should be developed. The general structure of a dc MG system is shown in Fig. 1. In general, MG consists of a number of parallel converters that should work in harmony. Local control functions of these converters typically cover the following: 1) current, voltage, and droop control for each unit; 2) source-dependent functions, e.g., MPPT for photovoltaic (PV) modules and wind turbines, or a state-of-charge (SoC) estimation for ESSes; 3) decentralized coordination functions, such as local adaptive calculation of VRs, distributed dc bus signaling (DBS), or power line signaling (PLS). At a global MG level, a digital communication-based coordinated control can be implemented to achieve advanced energy management functions. It can be realized either in a centralized or a distributed fashion, via central controller (CC) or sparse communication network, respectively. In case of distributed control, variables of interest are exchanged only between local controllers (LCs). Consensus algorithm can then be used to calculate either the average of all the variable values in distributed LCs or the exact value of any variable present in a specific LC. A detailed explanation on how this can be realized and a review of several consensus applications in dc MGs can be found in Section IV-C and references therein. Some of the functionalities that can be accomplished by using DCLs include secondary/tertiary control, real-time optimization, unit commitment, and internal operating mode changing (see Fig. 1 and Section IV for more details) [12].

From the communication perspective, overall control of dc MGs can be divided into the following three categories.

1) *Decentralized control:* DCLs do not exist and power lines are used as the only channel of communication.
2) *Centralized control:* Data from distributed units are collected in a centralized aggregator, processed and feedback commands are sent back to them via DCLs.
3) *Distributed control:* DCLs exist, but are implemented between units and coordinated control strategies are processed locally.

The basic configuration of each of these control structures is depicted in Fig. 2. A more detailed overview of the significant features of local and coordinated control strategies is provided in the following sections.

III. Local Control in DC MGs

As previously mentioned, the control framework of a dc MG consists in general of local and coordinated control levels. In this section, a local control level is discussed in detail. Basic functions which include current, voltage, and droop control are reviewed. Due to limited space and in an attempt to keep the scope of this paper as focused as possible, a review of MPPT and charging algorithms has been omitted here. More details on charging algorithms for batteries can be found in [45], while an

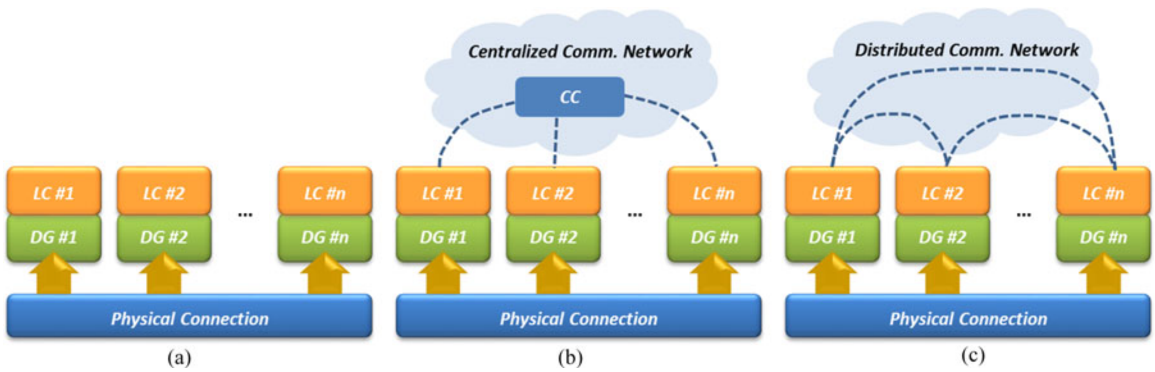

Fig. 2. Operating principles of basic control strategies. (a) Decentralized control. (b) Centralized control. (c) Distributed control.

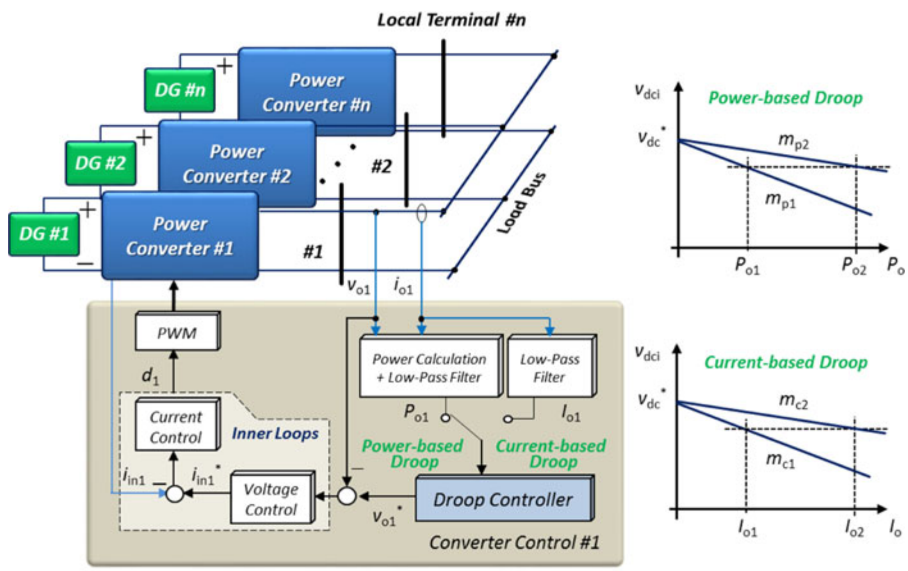

Fig. 3. Control diagram of interface converters based on power- or current-based droop control in dc MGs.

in-depth analysis of MPPT algorithms has been presented in a number of references, e.g., in [26] and [27].

As a backbone of a dc MG, the interface converters play an important role in efficient and reliable operation of the overall system. In order to ensure not only proper local operation, but also to enable coordinated interconnection between different modules in a dc MG, flexible local current and voltage control should be employed and accurate power sharing among parallel connected converters should be achieved. The basic local control diagram is shown in Fig. 3, including local current and voltage controllers, and a droop control loop.

For local dc current and voltage control systems in dc MGs, proportional-integral (PI) controllers are commonly used since they introduce zero steady-state error, can be easily tuned, and are highly robust [3]. However, the use of other types of controllers, such as proportional derivative (PD), fuzzy and boundary controllers has also been reported [43], [46]–[48]. PD controllers can be used to improve the phase margin (PM) of the system, but they do not eliminate steady-state error and also need to have high-frequency poles in order to attenuate the high-frequency noise. Hence, rather than appearing in a pure PD form, the derivative term in a PD controller is usually replaced by a high-pass digital filter. By combining the beneficial effects of PI and PD controllers, PID controllers can be employed. Fuzzy control is designed to emulate a human being's conclusion deduction process based on the stimulus he/she gets from the environment and his/her own embedded knowledge. In the engineering world, it can be defined as a knowledge-based control method that can simultaneously take advantage of both static and dynamic properties of the system [49]. For the purpose of local voltage and current regulation, fuzzy controllers can either be used as principal regulators that process the error signal [46] or in a series with feedback loops. To ensure fast convergence and extreme robustness, nonlinear control strategies based on state-dependent switching (e.g., boundary control in [48]) can be employed. They present simple implementation, but their detailed performance analysis can be quite complex. It should be noted that alternative control methods for dc MGs have recently drawn a lot of attention in the academic circles. However, their practical application should be elaborately justified by performing modeling, analysis, simulation, implementation, as well as a full cost-benefit analysis. For instance, increased production cost and lead time often prove to be too large of an obstacle for their deployment.

Droop control is commonly installed on top of inner loops, primarily for current sharing purposes. Fig. 3 demonstrates that either output power or output current can be selected as the feedback signal in droop control [3], [29]. For dc MGs with power-type load, output power can be used as droop feedback, as shown in (1). On the other hand, when current signal is used, as shown in (2), droop coefficient m_c can be regarded as a virtual internal resistance. In that case, the implementation and design of the parallel converter system in a dc MG can be simplified to some extent as the control law is linear [3]. The principle of current-based droop control was also extensively used in distributed power systems (DPS) for putting in parallel multiphase converters that supply computer CPUs. Here, droop control is commonly known as adaptive voltage positioning [50]–[52]. The calculations of references for voltage controller in the two aforementioned cases are as follows:

$$v_{\mathrm{DC}i}^{*} = v_{\mathrm{DC}}^{*} - m_{\mathrm{p}} \cdot P_{\mathrm{oi}} \quad (1)$$

$$v_{\mathrm{DC}i}^{*} = v_{\mathrm{DC}}^{*} - m_{c} \cdot i_{\mathrm{oi}} \quad (2)$$

where $v_{\mathrm{DC}i}^{*}$ is the output of the droop controller, i.e., the reference value of dc output voltage of the converter #*i*; v_{DC}^{*} is the rated value of dc voltage; m_p and m_c are the droop coefficients in power- and current-based droop controllers, while P_{oi} and i_{oi} are the output power and current of converter #*i*, respectively.

The values of droop coefficients have a profound effect on system stability and current sharing accuracy. In general, the higher the droop coefficients, the more damped system is and the better accuracy of current sharing. However, there exists a tradeoff since voltage deviation also increases. While stability is thoroughly discussed in Section V, more details on current sharing accuracy problem can be found in [23] and [53] and references therein.

It should be noted that, apart from its effects on current sharing accuracy and stability, droop control also has other system level repercussions. More precisely, with variations of droop coefficients, it is possible to regulate power injection/absorption of other droop-controlled converters by imposing desired voltage deviation in the common dc bus. For instance, in [23], the droop coefficients are designed and selected in order to achieve optimal coordinated operation and to minimize the output current sharing error. Meanwhile, the average current is calculated and added as a feedback signal term into the dc voltage reference to shift the *I–V* droop curve and reduce the large dc voltage deviation.

Finally, operating modes of converters can be changed according to the magnitude of voltage deviation imposed by droop [16], [28]. This feature, which can be considered an indirect way of control is broadly exploited in decentralized coordinated strategies which will be discussed in Section IV.

IV. Coordinated Control in DC MGs

Although the local interface converter control is an essential part of a dc MG, coordinated control should be implemented in order to achieve an intelligent control system with extended objectives. As already mentioned, depending on the means of communication between the interface converters, it can be realized either by using decentralized, centralized, or distributed control.

A. Decentralized Control

Decentralized coordination strategies are achieved exclusively by LCs, as shown in Figs. 1 and 2(a). In this section, we will review a number of decentralized methods that can coordinate the performance of multiple converters in dc MGs. The most common ones are DBS, adaptive adjustment of droop coefficients, and PLS. While their advantage is simplicity of control and independence from digital communication technology, they inherently have performance limitations due to lack of information from other units. Moreover, as these methods are invariably based on the interpretation of the voltage in the common dc bus, the accuracy of voltage sensors impacts their effectiveness and reliability.

Originally proposed in [16] and the follow-up in [15] and [54], DBS is the most prominent decentralized coordination method for dc MGs. By using the DBS approach, coordinated operation of different units in dc MGs is realized by imposing and identifying variations in the common dc bus voltage. The DBS principle is shown in Fig. 4, where three operating modes are developed and each one of them includes a different combination of operating statuses for PVs, ESSes, and ac grid interfacing converters. It can be seen from the figure that units are represented either as current sources/sinks or by Thevenin equivalent circuits, depending on their internal operating mode. The Thevenin circuit actually demonstrates that a given unit is in the droop control mode. The voltage source then corresponds to a voltage reference, while the series impedance corresponds to virtual impedance. The transitions between different modes are triggered by different preset dc bus voltage values.

Relying on the DBS principle and in the context of a smart nanogrid, a coordinated static operation of different energy sources, e.g., solar, wind, battery, is realized by using modified static *I–V* droop characteristics [55]. In [56], polyline style droop curves with multiple segments are used for battery energy storage units and grid-interfacing converters. Input power from wind, solar, and utility grid is controlled according to the SoC of battery by using a certain segment of the droop curve with different slopes. A multiterminal dc MG has been studied in [57], and droop control is categorized as pseudocritical, noncritical, and critical droop considering the characteristics and importance of different sources and loads. Here, droop curves are modified according to the voltage measured in a common dc bus. The segments of the droop curves represent different operation modes, i.e., voltage- or power-controlled modes. As these modes exhibit different dynamics, seamless mode transfer between them should be ensured in all possible cases. Another aggravating feature of this method is the fact that expandability with additional units is quite limited, since the settings of droop curves would have to be updated with every new unit. In [58], a frequency-shaped VR is employed and hybrid ESS with batteries and supercapacitors are used to simultaneously cope with low-frequency response and high-frequency power ripples. In [59], a flywheel ESS has been deployed for ramping

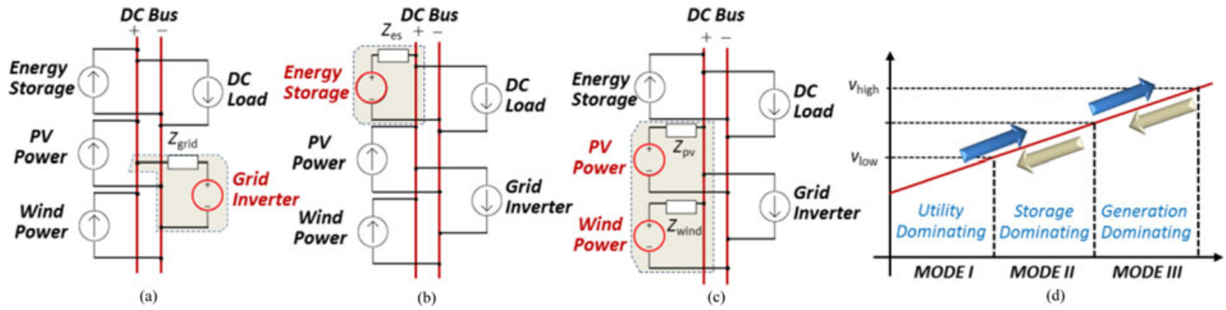

Fig. 4. Operation modes and basic principle of the DBS approach. (a) Utility dominating mode. (b) Storage dominating mode. (c) Generation dominating mode. (d) Basic principle of the DBS approach.

the response of a fast EV dc charging station. A power balancing strategy between the flywheel and grid tied converters has been designed using dc bus voltage as an exclusive communication medium. It should be noted that much better compensation of power imbalances can be achieved if fast digital communication is used, but this limits the expandability of the method [60].

To summarize the above, it can be concluded that DBS relies only on local information and does not need any other components other than interface converters. Therefore, it is a decentralized control method that is easy to implement. The main concern here is the selection of appropriate voltage levels which are needed to identify different operation modes [as shown in Fig. 4 (d)]. If the difference among the adjacent voltage levels is too large, the dc bus voltage fluctuation will exceed the acceptable range. Still, the difference among the voltage levels should not be too small since sensor inaccuracy and the dc bus voltage ripples could then prevent reliable identification of proper operating modes.

Adaptive calculation of droop coefficients is an extension of conventional droop control which does not consider change of operating modes. It is commonly used to balance SoC among multiple ESSes in order to avoid their overcharge or overdischarge. A dynamic SoC balancing method is realized in [28]–[30] by adjusting the droop coefficients according to SoC in both charging and discharging processes. Different functions have been proposed to control the SoC convergence speed and stability properties of the system at the same time. In [14], fuzzy control-based gain-scheduling droop control is proposed to dynamically adjust the droop coefficients and balance the SoC of each energy storage unit. In [47], the fuzzy control system is employed to obtain the VR which is used to balance the SoC and reduce the voltage deviation at the common dc bus. In [61], a modified curve of injected/extracted power set point versus SoC is proposed. The safe range of the SoC is selected as 10%–90%. By using this curve, the set point is kept constant when the SoC is in the range of 40%–60%. Meanwhile, if the SoC is in the range of 20%–40%, the set point is gradually reduced, and when it is in the range of 60%–80%, the set point is gradually increased. If the SoC comes to the range of 10%–20% or 80%–90%, which is near the lower or upper boundary, higher level supervisory control will be activated to determine the injected/output power. In [62], the power reference of each ESS is determined by considering the difference between the local voltage, and voltage at the PCC which is called global voltage. The global and local voltage signals are first sent to a dead band filter, and the output signals of the dead band filter are multiplied by different droop coefficients. Droop coefficients are selected to be proportional to the SoC of each ESS. By using this method, the impacts of the disturbances either at the PCC or locally are mitigated by modifying the output power of ESSes.

The method of adaptive droop coefficient calculation has been mainly used for power balancing of distributed ESSes, as shown above. The main limitation of the method is potential instability induced by improperly designed droop curves. To that end, there always exists a tradeoff between the permissible voltage deviation and stability properties of the system, i.e., higher voltage deviation is associated with the higher PM. It should also be noted that some of the SoC balancing methods mentioned above (see [61], [62]) were originally proposed for ac MGs. However, since the same principle can apply to dc MGs (in ac MGs, the frequency is normally used as a system level coordinating signal), they are also included here.

PLS is another decentralized method that can be deployed for coordinated control. In particular, sinusoidal signals of specific frequency are injected through amplifiers into the dc bus, allowing each device to send and receive information on its status, performance, history, or internal operational mode. Although PLS relies on digital communication, here it is categorized as decentralized since the power network is the only communication medium. It should be noted that in power systems literature, this particular way of communication is sometimes also referred to as power line communication [63]. REbus, an open standard for dc electricity distribution in homes, commercial buildings, campuses, and other settings, uses PLS as a primary communication carrier [64]. Alternative methods that exchange information between devices without using dedicated amplifiers were presented in [65] and [66]. Signals are generated by PWM of dc–dc converters in those works. They are injected in open loop in [66], whereas dedicated proportional-resonant controllers are used during injection periods in [65] to avoid the steady-state error in the dc bus.

In general, PLS is more complex to implement compared to other decentralized methods, such as DBS and adaptive droop. Moreover, it is commonly used only for changing operating modes or shutting corrupted components of the system, and it is not suitable for power sharing. However, as opposed to permanent voltage deviation in the common dc bus which is inherent for DBS and adaptive droop methods, sinusoidal signals are only periodically injected into the system. Therefore, the quality of the voltage waveform can be considered to some extent improved compared to other methods.

B. Centralized Control

Centralized control can be implemented in dc MGs by employing a CC and a digital communication network to connect it with sources and loads, as shown in the *DCL-based coordination control* window of Figs. 1 and 2(b). For small-scale dc MGs, each unit can be directly controlled by the CC that employs a high-bandwidth communication using a master/slave approach [67], [68]. However, for larger scale dc MGs, hierarchical control is often a preferred choice since it introduces a certain degree of independence between different control levels. It is more reliable as it continues to be operational even in case of failure of centralized control. Hierarchical control is achieved by simultaneously using local converter control and DCL-based coordinated control, which are separated by at least an order of magnitude in control bandwidth [3]. Coordinated functions can include secondary/tertiary regulation of dc voltage, power flow control, and different grid-interactive control objectives, such as unit commitment, changing operating modes, global optimization aimed at maximizing efficiency, minimizing operating cost, etc.

A centralized supervision control system is proposed in [13] in order to realize an adaptive operation of a dc MG-based data center. Eight operation modes are included in the control scheme and features of 23 transitions among them have been studied. In [69], a coordinated supervision control diagram for dc sustainable building comprised of PV arrays and EV chargers is proposed. The availability of the RESes and the real-time customer demands has been identified, and the optimal decisions are made based on the requirement of minimizing the operating cost. In [70], a hierarchical control system is deployed for a campus MG, and it is discussed how it can enhance the coordinated and optimal operation of on-site generation in relation to an ac-based system. In [71], a hierarchical control system is proposed for reliable and economical operation of standalone dc MGs. DC bus regulation and prioritizations for charging or discharging of batteries with a different SoC are analyzed. Meanwhile, load shedding for extreme operating conditions is studied. In [72], a hierarchical control diagram is employed on the interface converters between ac and dc buses and rectifier operation with ac to dc power flow is studied. The control objectives for local ac and dc voltages are achieved. At the same time, PCC voltage is restored in the secondary control level, and power exchange between the local dc MG and an external dc MG is realized in the tertiary control level. In [73], a multilayer supervision system is proposed focused on power balancing, load shedding, and constrained PV production with an aim of building an integrated system with PV and a battery. In [28], adaptive voltage droop control is proposed in the primary control level to balance the SoC. Meanwhile, a supervision control scheme in the higher level is developed to determine the transitions of different operation modes and to ensure coordinated recharging of multiple battery banks within the dc MG. Besides the control of a single dc MG, hierarchical control diagram can also be used for multiple dc MG clusters. In [74], a hierarchical control diagram with three control layers is employed not only to achieve the control objectives of the local MG, but also to optimize power distribution between different MG clusters.

It should be noted that centralized control provides the best foundation for the employment of advanced control functionalities since all relevant data can be collected and processed in a single controller. However, the most obvious disadvantage of this strategy is that it has a single point of failure. In particular, if the CC or any key communication link fails, the commands from/to the controller will not be transmitted and corresponding control objectives will likely not be achieved. For mission critical applications, redundant communication systems can be installed in order to reduce the possibility of failure, but this needs to be justified by a cost-benefit analysis. Another option to increase the reliability of the system is to combine decentralized and centralized control methods into a hierarchical control structure [28], [70]–[74]. In that case, basic functions of dc MGs can be retained even if the centralized controller fails.

C. Distributed Control

Distributed control indicates the control principle where central control unit does not exist and LCs communicate only among themselves through dedicated DCLs, as shown in Fig. 2(c). The main advantage of this approach is that the system can maintain full functionality, even if the failure of some communication links occurs, provided that communication network remains connected.[2] Therefore, distributed control is immune to single point of failure. The functionalities that can be achieved by this approach resemble those of centralized control and are also represented in the *DCL-based coordination control* window of Fig. 1.

However, in order to enable these functionalities, the information exchanged through DCLs first needs to be appropriately processed. In particular, information directly exchanged between LCs can contain only locally available variables. In other words, if the two units are not connected by a DCL, they do not have direct access to each other's data and their observation of the system is quite limited. In order to circumvent this problem and to make the level of awareness of an LC similar to that of a CC, a consensus algorithm can be used. In its basic form, a consensus algorithm is a simple protocol installed within every LC which continuously adds up all algebraic differences of some variable(s) of interest present in a given LC and those present in LCs adjacent to it. If we look at LC #*i*, this definition can also be expressed by the following equation:

$$\dot{x}_i(t) = \sum_{j \in N_i} [x_i(t) - x_j(t)] + b_i(t) \quad (3)$$

where $x_i(t)$ and $x_j(t)$ are the values of variables of interest in LC #*i* and LC #*j*, respectively. Here, j is iterated through the whole set of neighbors of LC #*i*, which is represented by N_i. Finally, $b_i(t)$ is an optional input bias of LC, which can be used to declare it as a virtual leader. It can be seen from (3) that $x_i(t)$

[2] For the exact definition and a more in-depth discussion of the connectivity of communication networks, see [76].

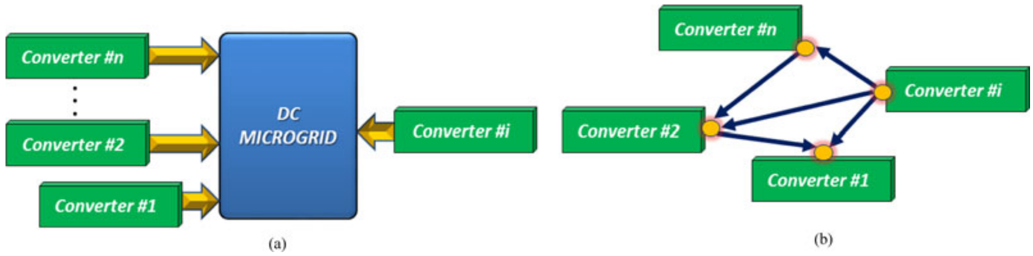

Fig. 5. Consensus algorithm in a dc MG based on a sparse communication graph. (a) Physical configuration of a dc MG. (b) Sparse communication graph.

is interactively adapted with respect to the values of its neighboring units. Likewise, variables in any other controller adapt with respect to the values of their own neighbors. Consequently, it can be analytically proved that, if the communication network is connected, all variable values will converge to a common average after a certain amount of time [75], [76]. Another option is to use a nonzero input bias in one of the LCs. In that case, variables of all other LCs will converge to his respective bias [77]. In either case, the ability of consensus to share information in such a manner has wider applicability than simple data averaging. For instance, if every LC has information on the number of other active LCs, an exact value of any specific variable can be calculated directly from the average.

The collective dynamics of communication system realized via consensus protocol can be represented by the following equation:

$$\dot{x}(t) = -\Theta \cdot x(t) \tag{4}$$

where $\Theta = [\theta_{\mathrm{ij}}]$ is the graph Laplacian of the network whose elements are defined as follows:

$$\theta_{\mathrm{ij}} = \begin{cases} -1, & j \in N_{\mathrm{i}} \\ |N_{\mathrm{i}}| & j = i \end{cases} \tag{5}$$

where $|N_i|$ denotes the number of neighbors of node #*i*. The topology of communication network is explicitly reflected by the graph Laplacian, and it is also possible to design weights of the respective matrix to control the convergence speed [78]. Fig. 5 shows the configuration of physical and an exemplary sparse communication network.

Recently, consensus algorithms have been deployed in a number of MG applications [22], [25], [79]. Some of them are reviewed hereinafter.

In [53], two additional PI controllers are employed to control the average dc voltage and average dc current obtained by the low-bandwidth communication-based consensus algorithm. Hence, the objectives of dc voltage restoration and output current sharing accuracy enhancement can be reached simultaneously. It should be noted that in this particular application, only static averaging was used since it was assumed that all units can communicate among themselves. A dynamic consensus protocol is employed in [22], where a noise-resilient dc voltage observer using the neighboring DG's information is developed to correct the local voltage set points. Also, a current regulator is employed to compare the local current with the neighbors' so that the current sharing error is removed. In [80], a straightforward application of a consensus algorithm is shown in a dc system with modular dc–dc converters. Each converter is selected as a node in the communication graph, and the configuration of the communication graph, i.e., the connection of dc–dc converters, can be selected arbitrarily. In comparison to [53], the methods proposed in [22] and [80] require only the neighbors' information, and the control diagram is implemented on a sparse communication graph across the MG, reducing the number of communication lines. Dynamic consensus algorithm was employed in [25] to optimize the global efficiency of a droop-controlled dc MG. In [81], it was used for voltage balancing of battery cells. Aside from the conventional principle of consensus algorithms, the leaderless consensus and leader–follower consensus are compared and analyzed.

In summary, it can be concluded that the distributed control can achieve information awareness comparable to that of the centralized control. Therefore, objectives, such as output current sharing, voltage restoration, global efficiency enhancement, SoC balancing, and others can be easily realized. In that sense, distributed control offers much wider functionalities than decentralized control, but remains protected from the single point of failure. Its main limitation is complexity of analytical performance analysis, i.e., assessment of convergence speed and stability margins, especially in nonideal environments characterized by communication time delays and measurement errors.

V. Stability Analysis and Stabilization Methods for DC MGs

In order to achieve safe and reliable MG performance, its dynamic stability needs to be ensured in all operating conditions. A typical cause of instability in dc MGs is impedance mismatch between lightly damped filters on the source side and tightly regulated power converters on the load side. These kinds of converters, often referred to as the constant power loads (CPLs), introduce a negative impedance characteristic in low frequency range that tends to oscillate with the output impedance of power supply filter [31], [82]. In practice, speed regulated motor drives and electronic loads may introduce such a destabilizing effect [32].

Averaging and linearization is the most common approach for modeling and analysis of switching power converters in dc MGs. The resulting small-signal models are valid for frequencies of up to around half of the switching frequency [82]. However, as the bandwidths of practical converters are typically in the range of one-tenth of the switching frequency, this method provides quite accurate analysis around the quiescent operating point. Models of individual components are assembled into a full-system model which is then typically broken down into two subsystems at an arbitrary dc point, i.e., a load subsystem and a source subsystem. Consequently, analytical expressions are derived for input impedance of the load Z_{in} and output impedance of the source Z_{s} subsystems. If each of the two subsystems are individually properly designed with good dynamic performance, the influence of their interaction can then be studied by looking into the ratio $Z_{\text{s}}/Z_{\text{in}}$, which is often referred to as the minor loop gain [31]. In particular, in order to preserve the stability, it is mandatory that minor loop gain meets the Nyquist stability criterion [31]. It should also be noted that, if the detailed information about source and load systems is not available and the respective impedances cannot be analytically constructed, they should be measured online [37], [83]–[88]. This is often the case in systems that are built by components provided by multiple vendors [33].

The impedance-based approach has one key advantage when compared to classical stability analysis tools used in large power systems [89]. It allows definition of straightforward stability criteria for every individual subsystem through convenient impedance specifications. First specification in that sense was proposed by Middlebrook in 1976 [31], and many others followed up on it in subsequent years [33]–[39]. This kind of individualized approach, which is discussed in detail in Section V-B, can largely simplify dynamic analysis and design of dc MGs.

Nevertheless, the stability results for impedance criteria rely heavily on the selection of the point in the system where it is broken into a load and source subsystems [39]. Moreover, the criteria provide only sufficient stability conditions and they implicitly assume unidirectional power flow which makes them inapplicable to systems where ESSes are used in the load side [90]. Finally, since only a minor loop gain is considered, the system should be well-tuned before the application of a filter [38]. In cases where these conditions are not met, a full-order state-space approach can be used as an alternative.

In order to provide a practical explanation of the stability phenomenon in dc MGs, a voltage regulated buck converter fed through a line filter on one side and supplying a resistive load on the other is taken as a demonstrative CPL example. Equations of interest corresponding to this configuration are presented in the following section. A number of different impedance specifications are then reviewed and elaborated. The section is concluded with a review of stabilization methods used in dc MGs

A. Dynamics of Regulated Power Supply

Fig. 6 shows a common dc bus realized by means of a power supply unit with a line filter to which a POL buck converter supplying a resistive load is connected. It should be noted that no generality is lost by analyzing this particular configuration, seeing as other types of CPLs would only exhibit different input impedance, whereas the analysis principles would remain the same.[3]

[3]For example, detailed procedures for obtaining input impedances for different types of dc–ac inverter-fed motor drives can be found in [42] and [96].

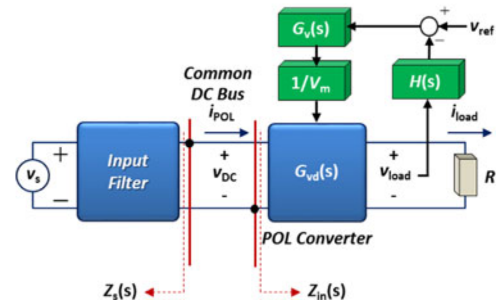

Fig. 6. Switching voltage regulator system supplied by source through a filter.

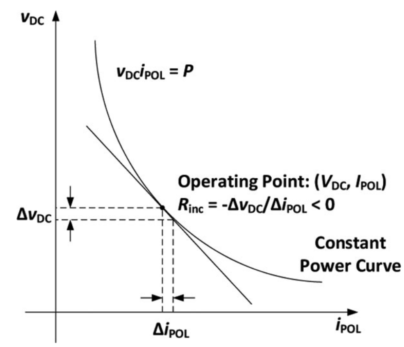

Fig. 7. Negative incremental impedance induced by POL converters.

The role of the line filter is twofold, i.e., it flattens the current drawn from the supply side and attenuates high-frequency variations at the input terminals of POL converter. However, while providing these two important functionalities, the supply side filter brings in additional dynamics which might induce undesirable interactions with the POL converter if the system is not properly designed.[4]

The voltage controller of the POL converter is tuned to adjust the duty ratio so as to try and keep the voltage on resistor constant regardless of any voltage changes in the common dc bus. If voltage control loop works perfectly, the voltage, and, therefore, the power on resistor will maintain constant value. Therefore, in case when v_{DC} decreases, i_{POL} would automatically increase in order to maintain that constant power, causing the incremental resistance seen from the dc bus side appearing with a negative incremental value. It can be expressed in (6) and also seen in Fig. 7

$$R_{\text{inc}} = \frac{\partial v_{\text{DC}}}{\partial i_{\text{POL}}} = \frac{\partial}{\partial i_{\text{POL}}}\left(\frac{P}{i_{\text{POL}}}\right) = -\frac{P}{I_{\text{POL}}^2} \tag{6}$$

where v_{DC} and i_{POL} are the output voltage and current of the POL converter, P is the constant power consumed on the resistor R, and I_{POL} is the steady-state value of i_{POL}.

However, ideal voltage controllers do not exist, in practice, and the equation above is, hence, valid only at frequencies well

[4]We limit our discussion here to a single supply source and a single POL converter. However, the same analysis can be applied if there are multiple sources/loads by considering their aggregated characteristics in the analysis (see, i.e., [90]).

below the crossover frequency of the system's loop gain. Conversely, when going toward and above the crossover frequency, the gain of voltage controller declines, causing the change of effective impedance from negative to positive [31], [82]. Therefore, it is of instrumental importance to obtain exact analytical expression for closed-loop input impedance of POL converter in order to describe the dynamics of a load subsystem and quantify its interaction with the supply side.

Closed-loop input impedance of the POL converter depends on the configuration of the load, converter filter, and loop gain of the converter control circuit. As already mentioned, it consists of two portions: one that dominates in the low-frequency region and other at high frequencies. Loop gain binds these two parts together by defining the magnitude and phase response in between. Low-frequency impedance is a negative resistor that corresponds to the value given in (6), while the high frequency one is simply an open-loop impedance of the POL converter filter. Following the nomenclature in [82], these impedances are designated as $Z_N(s)$ and $Z_D(s)$, respectively, and can be expressed as follows if a buck POL converter is considered:

$$Z_N(s) = R_{\rm inc} = -\frac{R}{D^2} \tag{7}$$

$$Z_D(s) = \frac{R}{D^2}\frac{\left(1+s\frac{L}{R}+s^2LC\right)}{(1+sRC)} \tag{8}$$

where *R*, *L,* and *C* are resistive load, inductance, and capacitance of the converter, while *D* is the duty ratio at a given operating point. The corresponding quantities for other types of basic dc–dc converters can be found in [82].

Loop gain *T*(s) is a product of the transfer functions (TFs) representing different elements in the forward and feedback paths of the control system. Considering the voltage regulated POL converter in Fig. 6, *T*(s) can be represented as

$$T(s) = \frac{H(s)G_c(s)G_{vd}(s)}{V_m} \tag{9}$$

where *H*(*s*) is the sensor gain from feedback path, $G_c(s)$ is the TF of voltage controller, $G_{vd}(s)$ is the TF describing the relation between converter duty ratio and output voltage, and $1/V_m$ is the PWM gain. These quantities can be used to give an expression that describes the closed-loop input impedance [31], [82], [91]

$$\frac{1}{Z_{\rm in}(s)} = \frac{1}{Z_{\rm N}(s)}\frac{T(s)}{1+T(s)} + \frac{1}{Z_{\rm D}(s)}\frac{1}{1+T(s)} \tag{10}$$

It is visible from the above equation that input impedance follows $Z_N(s)$ at low frequencies, where magnitude of *T*(s) is high, whereas $Z_D(s)$ becomes dominant at high frequencies where $T(s)$ drops down in magnitude. It should be noted that $Z_{\rm in}(s)$ is an independent quantity in the circuit and remains unaffected by the filter configuration at the supply side. Likewise, the output impedance of supply filter $Z_s(s)$ is independent from $Z_{\rm in}(s)$. In the following paragraphs, it will be shown how the stability properties of the system can be examined by looking into interaction of these two impedances.

There are essentially three independent inputs to the POL system; control input $\hat{v}_{\rm ref}$, load current $\hat{i}_{\rm load}$, and supply side

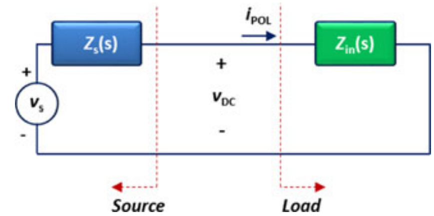

Fig. 8. Thevenin equivalent source and load converter model.

voltage $\hat{v}_{\rm DC}$. The reason why caps are put on top of these inputs is that the model considered here is linearized around operating point and we are interested only with small signal variations. The output voltage variation in open loop can be described by linear combination of inputs, where $G_{vd}(s)$, $G_{vg}(s)$, and $Z_{\rm out}(s)$ represent corresponding open-loop TFs (see [82] for details). Once the control loop is closed, control input becomes a variable in the system calculated by the compensator $G_c(s)$ from the voltage error. Then, voltage variation on the load side can be described as [82]

$$\hat{v}_{\rm load} = \hat{v}_{\rm ref}\frac{1}{H(s)}\frac{T(s)}{1+T(s)} + \hat{v}_{\rm DC}\frac{G_{vg}(s)}{1+T(s)} - \hat{i}_{\rm load}\frac{Z_{\rm out}(s)}{1+T(s)}. \tag{11}$$

When the supply voltage $\hat{v}_{\rm DC}$ is provided through the input filter, TFs in (11) experience certain modifications. Modification of the line transmission characteristic can be explained with an equivalent Thevenin circuit shown in Fig. 8. In that sense, by applying a voltage divider formula, one can establish the relationship between $\hat{v}_{\rm s}$ and $\hat{v}_{\rm DC}$

$$\hat{v}_{\rm DC} = \frac{Z_{\rm in}(s)}{Z_{\rm in}(s)+Z_s(s)}\hat{v}_s = \frac{1}{1+\frac{Z_s(s)}{Z_{\rm in}(s)}}\hat{v}_s = \frac{1}{1+T_{\rm MLG}(s)}\hat{v}_s. \tag{12}$$

It can be seen from (12) how the stability of the whole system is determined by the relation $Z_s(s)/Z_{\rm in}(s)$, which is in the literature commonly referred to as the minor loop gain or $T_{\rm MLG}(s)$ [31], [90], which can be expressed as

$$T_{\rm MLG}(s) = \frac{Z_{\rm s}(s)}{Z_{\rm in}(s)} = \frac{Z_{\rm s}(s)}{Z_{\rm N}(s)}\frac{T(s)}{1+T(s)} + \frac{Z_{\rm s}(s)}{Z_{\rm D}(s)}\frac{1}{1+T(s)} \tag{13}$$

On the other hand, the addition of output impedance $Z_s(s)$ also affects the loop gain of the converter. This change can be analytically calculated by deploying the extra element theorem [92]

$$G_{vd,{\rm filt}}(s) = G_{vd}(s)\frac{1+\frac{Z_s(s)}{Z_N(s)}}{1+\frac{Z_s(s)}{Z_D(s)}}. \tag{14}$$

Then, by incorporating $G_{vd,{\rm filt}}(s)$ instead of $G_{vd}(s)$ in (9), one can obtain modified *T*(*s*). Next section builds upon the theoretical foundation presented here and reviews some common impedance specifications that ensure stable dc power systems.

B. Impedance Specifications

If an idealized representation of a CPL via negative resistance is considered, one can easily derive impedance specification for

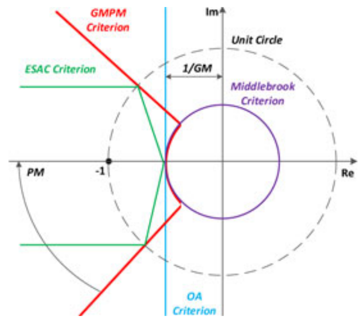

Fig. 9. Most prominent impedance criteria.

stability by preventing the poles of the system from entering the right-half plane. Assuming a simple *LC* filter configuration at the supply side, the stability condition for that case can be defined as follows:

$$\frac{L}{|R_{\mathrm{inc}}|} \leq R_{\mathrm{L}} C \tag{15}$$

where *L*, R_L, and *C* are inductance, resistance in series with inductance, and capacitance of buck converter filter. However, although (15) is very intuitive for demonstrating how different parameters affect the stability, it is valid only at low frequencies.

Middlebrook was first to recognize this shortcoming, and observing the complete dynamic characteristics of POL converter, defined a criterion by which the supply side filter would not have any influence on the dynamics of the system [31]

$$\begin{cases} \left|\frac{Z_{\mathrm{s}}}{Z_{\mathrm{N}}}\right| \ll 1 \\ \left|\frac{Z_{\mathrm{s}}}{Z_{\mathrm{D}}}\right| \ll 1. \end{cases} \tag{16}$$

With this pair of inequalities, it is ensured that the system dynamics are virtually unaffected by the input filter since $T_{\mathrm{MLG}}(s)$ disappears [see (13)]. In order to satisfy (16), one needs to have detailed information on the load to derive Z_N and Z_D. If this is not available, then Z_{in} can be determined by direct online measurement and a simpler but more restrictive criterion can then be applied

$$|T_{\mathrm{MLG}}| = \frac{|Z_s|}{|Z_{\mathrm{in}}|} \ll 1. \tag{17}$$

A relaxation of (17) to achieve required gain margin (GM) rather than aiming for unaltered system dynamics can also be employed

$$|T_{\mathrm{MLG}}| = \frac{|Z_s|}{|Z_{\mathrm{in}}|} \leq \frac{1}{\mathrm{GM}}. \tag{18}$$

Circle defined by (18) is plotted in polar coordinates in Fig. 9. The area outside the respective circle represents a forbidden region for the minor loop gain.

It should be noted that the Middlebrook criterion considers only magnitudes of impedances and it was soon realized that it is overly conservative since the forbidden region in the *s*-plane occupies much of the area, which is irrelevant from stability point of view. This kind of restriction can increase the cost of the design without improving system performance. In attempt to circumvent this obstacle, a number of alternatives were proposed in order to open up more of the *s*-plane for the minor loop gain [33]–[39]. For comparison, boundaries of three prominent specifications, i.e., the energy source analysis consortium (ESAC) criterion [39], gain margin and phase margin (GMPM) criterion [36], and opposing argument (OA) criterion [37] are plotted in Fig. 9 along with the Middlebrook criterion.

In the GMPM criterion [36], the forbidden region was defined by the following relation:

$$\begin{cases} |Z_s| - |Z_{\mathrm{in}}| > -\mathrm{GM[dB]} \\ 180^\circ - \mathrm{PM}_1 < \angle Z_s - \angle Z_{\mathrm{in}} < 180^\circ + \mathrm{PM}_2. \end{cases} \tag{19}$$

By keeping Z_s/Z_{in} out of this forbidden region, small-signal system stability can be ensured with a specified GMPM. Typically they are chosen as 6 dB and 60°, respectively. This specification was extended in [37] by the OA criterion, where a system with multiple loads was considered. In order to facilitate the application of one general criterion to multiple loads, the following system level relation was proposed as the objective:

$$\mathrm{Re}\left(\frac{Z_s}{Z_{\mathrm{in}}}\right) \geq -\frac{1}{2}. \tag{20}$$

Then, it was shown that every individual load #*i* with power $P_{\mathrm{load}i}$ needs to satisfy (21) and (22) so that the system level criterion (20) is met

$$\mathrm{Re}\left(\frac{Z_{\mathrm{s}}}{Z_{\mathrm{in}i}}\right) \geq -\frac{1}{2} \cdot \frac{P_{\mathrm{load}i}}{P_{\mathrm{source}}} (i = 1, 2, \ldots, n) \tag{21}$$

$$-90^\circ - \Phi_i < \angle Z_s - \angle Z_{\mathrm{in}i} < 90^\circ + \Phi_i. \tag{22}$$

The ESAC criterion has the smallest forbidden region and suffers the least from different grouping of the sources [39]. The ESAC defines the boundary of the forbidden region by two symmetrical line segments; they start at infinity, go in parallel with the real axis, and, then, bend at the unit circle to connect at the point $s = -1/\mathrm{GM}$. What makes this criterion different from others is that it is constructed in reverse fashion, i.e., the analytical specification for impedance is reconstructed from the graph. In that sense, the ESAC criterion is somewhat more difficult to use when compared to others.

C. *Stabilization Strategies*

The common way of meeting impedance criteria is to smooth the resonant peak of the input filter by adding physical resistors in series and/or parallel with respective inductors and capacitors [31], [40], [82], [93]. This approach is commonly referred to as passive stabilization, and an extensive overview of these kinds of techniques for dc systems can be found in [82]. However, adding physical damping elements introduces dissipative losses to the system. Therefore, researcher has come up with active damping solutions where stabilization can be achieved only by modifying the POL converter or source converter control loops. A review of several prominent active damping methods is provided next.

Active damping can be divided into small- and large-signal strategies. The basic principle in small-signal stabilization strategies is the introduction of linear feedback control loop that modifies the loop gain of the system *T*(*s*) and produces

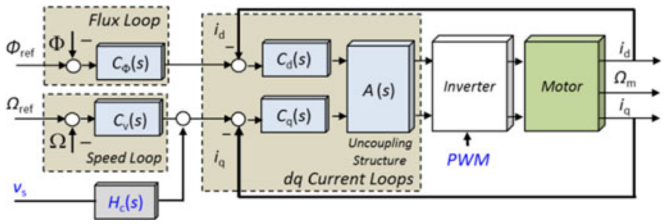

Fig. 10. Field-oriented control of inverter-motor-drive system with oscillation compensation block.

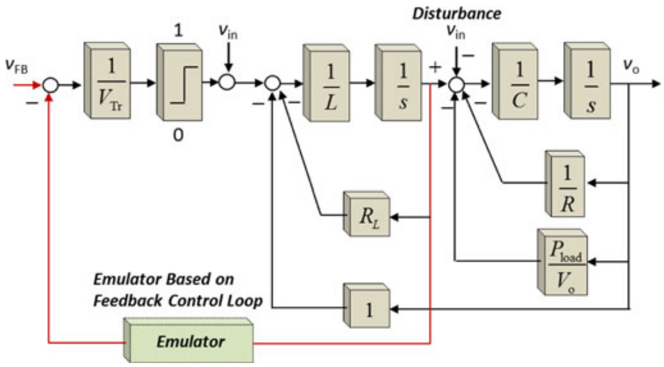

Fig. 11. Linear feedback-based damping method for dc MGs with CPLs.

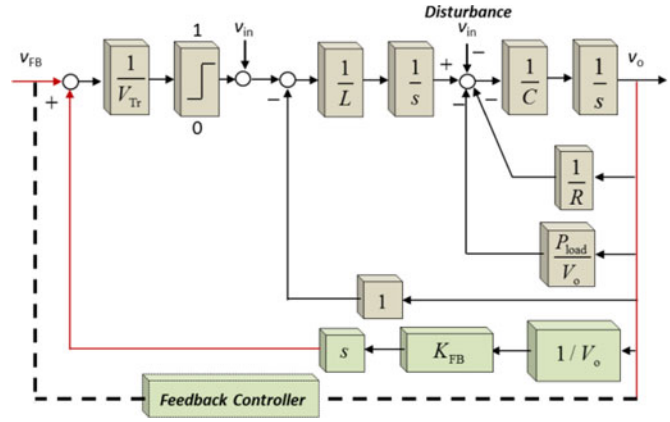

Fig. 12. Block diagram representation of a buck converter with the loop-cancellation technique implemented.

similar damping effects as the real damping elements, but without sacrificing the efficiency [20], [94], [95]. From the minor loop gain specification viewpoint, active damping is able to shape either the closed-loop impedance of the POL converter $Z_{\rm in}(s)$ or output impedance of power supply Z_s. One example of shaping $Z_{\rm in}$ is shown in [42] where the proposed stabilization block is a proportional compensator followed by a bandpass filter. This block takes dc-link voltage as input and adds its output to speed-control calculated current reference in q-axis. The influence of this control loop, which is shown in Fig. 10, on $Z_{\rm in}(s)$ for the PMSM drive is studied in detail, while proportional gain of the stabilizer is selected by inspecting Nyquist diagrams. Similar approach is adopted for brushless dc motor drive in [96], but the root locus method is used to shape $Z_{\rm in}(s)$.

Active damping strategies for basic types of dc–dc converters supplying CPL are given in [20]. Here, the principle of the proposed damping method is shown in Fig. 11. By examining the model of the whole system, it is shown how this control loop improves the damping of the system in a similar way as a physical resistor. Although the authors do not explicitly state it, this approach allows them to basically smooth out the resonant peak of the output impedance $Z_{\rm s}$. Also, it is interesting to notice that this VR emulator is equivalent to droop controller, although it is used exclusively for active damping purposes rather than for current sharing between multiple sources. In [94], it is shown how, with an appropriate selection of feedback loops, the resistors, inductors, and capacitors can be emulated.

In [41], active damping methods based on linear feedback loops are implemented in the interfacing converter which links the dc MG and external ac grid. The output impedance of this interface converter is reshaped to obtain the damping function. Three kinds of approaches are proposed by injecting the active damping signals into the outer, intermediate, and inner loops, respectively.

A drawback of linear feedback stabilization techniques is the fact that they are valid only for analyzed operating point and added feedback loop may not operate satisfactorily outside its neighborhood. Therefore, for the drives where power of CPL varies considerably, it is sometimes preferable to develop an adaptive stabilization strategy. In that sense, there are three options: 1) nonlinear analysis for a linear controller design; 2) nonlinear analysis for a nonlinear controller design; 3) linear analysis for a nonlinear controller design.

In the first option, the nonlinear analysis tools are used to obtain valid conditions for global stability realized by linear controllers. In that sense, it was proved that with the help of a nonlinear passivity concept, a PD controller can ensure global stability of a dc MG, given that the PD terms are properly selected [97]. The concept of a virtual capacitor is applied in [44], and the concrete capacitance that ensures stability is found in the Takagi–Sugeno model.

In the second option, the large-signal stability is ensured by applying nonlinear controllers. In [43] and [48], a geometric-based nonlinear method, referred to as the boundary control is employed to drive the source converter which feeds CPL to a desired operating point. This technique tracks the state variables of the source converter in order to select a boundary at which the switching occurs. Then, the switching happens every time when the trajectories of selected state variables cross the boundary. A quadratic voltage controller stabilizing CPL is presented in [98]. The results showed that a permanent-magnet brushless AC motor can be stabilized by this strategy when compared to the simple linear voltage regulator. Rahimi *et al.* [99] deploy a nonlinear feedback loop shown in Fig. 12 and refer to it as a loop-cancellation technique. The loop is placed in parallel with the classical voltage feedback path in order to achieve zero steady-state error and damping at the same time. Root locus technique is used for finding the optimal parameters.

In the third option, Tahim *et al.* [100] propose a linear stability assessment using the Jacobian matrix in order to test the proposed nonlinear controller. To that end, sliding mode control supplemented with the washout filter is employed, and its proper operation is ensured by generating the stability conditions from the Jacobian matrix.

VI. Concluding Remarks and Future Trends

In this paper, we have reviewed the current status in dc MG control, dynamic stability analysis, and stabilization techniques. Local control of converters plays an instrumental role not only in achieving voltage and current regulation, but also in enabling coordinated control strategies which are integrated in a higher control level and give commands to local level according to imposed control objectives.

Targeting at a single converter, a PI, PD, PID, boundary, fuzzy, or other types of controllers can be deployed to ensure the power quality of local voltage and current. Each one of them has some specific advantages and disadvantages as discussed earlier in this paper. Due to the fact that they are easily adjustable and have fast lead time, PID-based LCs are still the most frequently used. On the other hand, for paralleling multiple converters within a dc MG, accuracy of output current or power sharing is instrumental. Among various load sharing methods, droop control and its variants are most widely used and have been intensively studied in the past years. Meanwhile, ESSes are required in MGs to mitigate the power fluctuation of the intermittent output power of RESes, and their safe and reliable operation should be guaranteed.

Relying on communication between units within the MG, three main coordinated control methods can be distinguished, i.e., decentralized, centralized, and distributed control. Decentralized control schemes use power lines as a communication medium. The most popular decentralized control method is called DBS. It is a variant of droop control which is implemented based on dc bus voltage variation through which every unit can independently determine when to change its internal operation mode. Another variation of conventional droop control is adaptive calculation of droop coefficients. However, the change of operating modes is not taken into consideration here, but it is normally used for balancing SoCs of multiple ESSes within the system. An alternative decentralized strategy is PLS which is based on injecting and interpreting sinusoidal voltage waveforms in the common dc bus. Unlike DBS and adaptive droop, which are based on continuous deviation of the common dc bus voltage, PLS injects signals only when a change of operating mode or reconfiguration in the system are required. Although this method allows operation under nominal voltage in all conditions, PLS is not suitable for current sharing purposes.

Centralized control schemes are based on a CC which communicates with all other units through dedicated DCLs. Supervisory system is deployed to realize advanced functions, such as unit commitment and global optimization or to determine proper operation modes for each unit in dc MGs, In addition, in order to achieve secondary/tertiary control of a dc MG with multiple units, a hierarchical control diagram can be employed. Centralized control offers the highest level of flexibility for achieving advanced functionalities, but is a system with an inherent single point of failure.

Distributed control methods structurally resemble the decentralized ones, but can achieve similar functions as centralized methods since they also involve digital communication. They collectively gather data among themselves and process it either through consensus-based algorithms or directly. By consensus principle, every LC can obtain knowledge about the system comparable to centralized control, but with a time delay required for convergence. In general, distributed control has enhanced reliability compared to centralized control, since there is no single point of failure. However, rigorous mathematical analysis of distributed control strategies remains a challenging research topic, especially in nonideal environments (variant communication delays, measurement noise, and imperfect electrical control systems) which we commonly encountered in real life.

Loads in dc MGs are often active, electronically regulated by a specific converter, and can be considered CPLs in the low-frequency region where their bandwidth is sufficiently high to make the consumed power independent of the bus voltage variations. This type of characteristic brings in stability concerns since CPLs behave as negative resistance oscillators in that region. In this respect, a detailed elaboration of frequency characteristics of electronically regulated loads has been presented, and it has been shown how the relationship between effective impedances of source and load subsystems determines the stability of the whole system. Several impedance specification for this relationship, also referred to as the minor loop gain, has been reviewed before presenting a number of stabilization methods that can help achieve these specifications and good dynamic performance of dc MGs in general.

DC MG control area will continue to evolve rapidly in the coming years. Regarding local control, one of the important research focuses will be the mitigation of adverse dynamic effects introduced by CPLs using linear and nonlinear control techniques. On the coordinated control level, the design of centralized controllers for optimal demand response in variable grid price scenario presents a significant future challenge. New versions of DBS, PLS, and adaptive droop decentralized control methods will attempt to increase their intelligence level. With regard to that, extended functionalities, such as differentiation of loads according to their supply priority or sources in line with their specific characteristics will be implemented. Distributed control strategies which have recently spurred a great amount of interest in the dc MG research community, will also continue its development. In particular, as opposed to advocated advantages in terms of increased redundancy and reliability in relation to centralized control, a better understanding of their implications on the stability of the overall system will need to be obtained. Development of impedance-based models of a wide class of a variable speed motor drives is yet another prominent research topic. Due to their complex control architecture, it is highly desirable to develop simplified models which can represent the dynamics of the drive with acceptable accuracy. These impedance models can then be used either for simulation of larger scale dc MGs (with reduced computational burden) or for fast stability verification using some of the impedance criteria that were reviewed in this paper.

References

[1] A. Ipakchi and F. Albuyeh, “Grid of the future,” *IEEE Power Energy Mag.*, vol. 7, no. 2, pp. 52–62, Mar./Apr. 2009.

[2] R. H. Lasseter, “MicroGrids,” in *Proc. IEEE Power Eng. Soc. Winter Meet.*, 2002, pp. 305–308.

[3] J. M. Guerrero, J. C. Vasquez, J. Matas, L. G. de Vicuna, and M. Castilla, "Hierarchical control of droop-controlled AC and DC microgrids—A general approach toward standardization," *IEEE Trans. Ind. Electron.*, vol. 58, no. 1, pp. 158–172, Jan. 2011.

[4] N. Pogaku, M. Prodanovic, and T. C. Green, "Modeling, analysis and testing of autonomous operation of an inverter-based microgrid," *IEEE Trans. Power Electron.*, vol. 22, no. 2, pp. 613–625, Mar. 2007.

[5] J. M. Guerrero, M. Castilla, J. C. Vasquez, J. Matas, and L. G. de Vicuna, "Control strategy for flexible microgrid based on parallel line-interactive UPS systems," *IEEE Trans. Ind. Electron.*, vol. 56, no. 3, pp. 726–736, Mar. 2009.

[6] R. Majumder, B. Chaudhuri, A. Ghosh, G. Ledwich, and F. Zare, "Improvement of stability and load sharing in an autonomous microgrid using supplementary droop control loop," *IEEE Trans. Power Syst.*, vol. 25, no. 2, pp. 796–808, May 2010.

[7] K. De Brabandere, B. Bolsens, J. den Keybus, A. Woyte, J. Driesen, and R. Belmans, "A voltage and frequency droop control method for parallel inverters," *IEEE Trans. Power Electron.*, vol. 22, no. 4, pp. 1107–1115, Jul. 2007.

[8] J. A. Peas Lopes, C. L. Moreira, and A. G. Madureira, "Defining control strategies for microgrids islanded operation," *IEEE Trans. Power Syst.*, vol. 21, no. 2, pp. 916–924, May 2006.

[9] J. Rocabert, A. Luna, F. Blaabjerg, and P. Rodríguez, "Control of power converters in AC microgrids," *IEEE Trans. Power Electron.*, vol. 27, no. 11, pp. 4734–4749, Nov. 2012.

[10] Y. W. Li and C.-N. Kao, "An accurate power control strategy for power-electron.-interfaced distributed generation units operating in a low-voltage multibus microgrid," *IEEE Trans. Power Electron.*, vol. 24, no. 12, pp. 2977–2988, Dec. 2009.

[11] Q.-C. Zhong, "Robust droop controller for accurate proportional load sharing among inverters operated in parallel," *IEEE Trans. Ind. Electron.*, vol. 60, no. 4, pp. 1281–1290, Apr. 2013.

[12] T. Dragicevic, J. C. Vasquez, J. M. Guerrero, and D. Skrlec, "Advanced LVDC electrical power architectures and microgrids: A step toward a new generation of power distribution networks," *IEEE Electrif. Mag.*, vol. 2, no. 1, pp. 54–65, Mar. 2014.

[13] D. Salomonsson, L. Soder, and A. Sannino, "An adaptive control system for a DC microgrid for data centers," *IEEE Trans. Ind. Appl.*, vol. 44, no. 6, pp. 1910–1917, Nov./Dec. 2008.

[14] H. Kakigano, Y. Miura, and T. Ise, "Distribution voltage control for DC microgrids using fuzzy control and gain-scheduling technique," *IEEE Trans. Power Electron.*, vol. 28, no. 5, pp. 2246–2258, May 2013.

[15] K. Sun, L. Zhang, Y. Xing, and J. M. Guerrero, "A distributed control strategy based on DC bus signaling for modular photovoltaic generation systems with battery energy storage," *IEEE Trans. Power Electron.*, vol. 26, no. 10, pp. 3032–3045, Oct. 2011.

[16] J. Schonberger, R. Duke, and S. D. Round, "DC-bus signaling: A distributed control strategy for a hybrid renewable nanogrid," *IEEE Trans. Ind. Electron.*, vol. 53, no. 5, pp. 1453–1460, Oct. 2006.

[17] P. Karlsson and J. Svensson, "DC bus voltage control for a distributed power system," *IEEE Trans. Power Electron.*, vol. 18, no. 6, pp. 1405–1412, Nov. 2003.

[18] R. S. Balog and P. T. Krein, "Bus selection in multibus DC microgrids," *IEEE Trans. Power Electron.*, vol. 26, no. 3, pp. 860–867, Nov. 2011.

[19] R. S. Balog, "Autonomous local control in distributed DC power systems," Ph.D. dissertation, Dept. Electr. Comput. Eng., Univ. Illinois Urbana-Champaign, Champaign, IL, USA, 2006.

[20] A. M. Rahimi and A. Emadi, "Active damping in DC/DC power electronic converters: A novel method to overcome the problems of constant power loads," *IEEE Trans. Ind. Electron.*, vol. 56, no. 5, pp. 1428–1439, May 2009.

[21] B. K. Johnson, R. H. Lasseter, F. L. Alvarado, and R. Adapa, "Expandable multiterminal DC system based on voltage droop," *IEEE Trans. Power Del.*, vol. 8, no. 4, pp. 1926–1932, Oct. 1993.

[22] V. Nasirian, S. Moayedi, A. Davoudi, and F. Lewis, "Distributed cooperative control of DC Microgrids," *IEEE Trans. Power Electron.*, vol. 30, no. 4, pp. 2288–2303, Apr. 2015.

[23] S. Anand, B. G. Fernandes, and J. M. Guerrero, "Distributed control to ensure proportional load sharing and improve voltage regulation in low-voltage DC microgrids," *IEEE Trans. Power Electron.*, vol. 28, no. 4, pp. 1900–1913, Apr. 2013.

[24] Q. Shafiee, T. Dragicevic, F. Andrade, J. C. Vasquez, and J. M. Guerrero, "Distributed consensus-based control of multiple DC-microgrids clusters," in *Proc. IEEE Annu. Conf. Ind. Electron. Soc.*, 2014, pp. 2056–2062.

[25] L. Meng, T. Dragicevic, J. M. Guerrero, and J. C. Vasquez, "Dynamic consensus algorithm based distributed global efficiency optimization of a droop controlled DC microgrid," in *Proc. IEEE Int. Energy Conf.*, 2014, pp. 1276–1283.

[26] E. Koutroulis and K. Kalaitzakis, "Design of a maximum power tracking system for wind-energy-conversion applications," *IEEE Trans. Ind. Electron.*, vol. 53, no. 2, pp. 486–494, Apr. 2006.

[27] B. Subudhi and R. Pradhan, "A comparative study on maximum power point tracking techniques for photovoltaic power systems," *IEEE Trans. Sustainable Energy*, vol. 4, no. 1, pp. 89–98, Jan. 2013.

[28] T. Dragicevic, J. M. Guerrero, J. C. Vasquez, and D. Skrlec, "Supervisory control of an adaptive-droop regulated DC microgrid with battery management capability," *IEEE Trans. Power Electron.*, vol. 29, no. 2, pp. 695–706, Feb. 2014.

[29] X. Lu, K. Sun, J. M. Guerrero, J. C. Vasquez, and L. Huang, "Double-quadrant state-of-charge-based droop control method for distributed energy storage systems in autonomous DC microgrids," *IEEE Trans. Smart Grid*, vol. 6, no. 1, pp. 147–157, Jan. 2015.

[30] X. Lu, K. Sun, J. M. Guerrero, J. C. Vasquez, and L. Huang, "State-of-charge balance using adaptive droop control for distributed energy storage systems in DC microgrid applications," *IEEE Trans. Ind. Electron.*, vol. 61, no. 6, pp. 2804–2815, Jun. 2014.

[31] R. D. Middlebrook, "Input filter considerations in design and application of switching regulators," in *Proc. IEEE Ind. Appl. Soc. Annu. Meet.*, 1976, pp. 366–382.

[32] A. Emadi, A. Khaligh, C. H. Rivetta, and G. A. Williamson, "Constant power loads and negative impedance instability in automotive systems: Definition, modeling, stability, and control of power electronic converters and motor drives," *IEEE Trans. Veh. Technol.*, vol. 55, no. 4, pp. 1112–1125, Jul. 2006.

[33] S. D. Sudhoff and J. M. Crider, "Advancements in generalized immittance based stability analysis of DC power electronics based distribution systems," in *Proc. IEEE Electr. Ship Technol. Symp.*, 2011, pp. 207–212.

[34] A. Riccobono and E. Santi, "A novel passivity-based stability criterion (PBSC) for switching converter DC distribution systems," in *Proc. IEEE 27th Annu. Appl. Power Electron. Conf. Expo.*, 2012, pp. 2560–2567.

[35] M. Belkhayat, R. Cooley, and A. Witulski, "Large signal stability criteria for distributed systems with constant power loads," in *Proc. IEEE Annu. Power Electron. Spec. Conf.*, 1995, vol. 2, pp. 1333–1338.

[36] C. M. Wildrick, F. C. Lee, B. H. Cho, and B. Choi, "A method of defining the load impedance specification for a stable distributed power system," *IEEE Trans. Power Electron.*, vol. 10, no. 3, pp. 280–285, May 1995.

[37] X. Feng, J. Liu, and F. C. Lee, "Impedance specifications for stable DC distributed power systems," *IEEE Trans. Power Electron.*, vol. 17, no. 2, pp. 157–162, Mar. 2002.

[38] X. Wang, R. Yao, and F. Rao, "Three-step impedance criterion for small-signal stability analysis in two-stage DC distributed power systems," *IEEE Power Electron. Lett.*, vol. 1, no. 3, pp. 83–87, Sep. 2003.

[39] S. D. Sudhoff, S. F. Glover, P. T. Lamm, D. H. Schmucker, and D. E. Delisle, "Admittance space stability analysis of power electronic systems," *IEEE Trans. Aerosp. Electron. Syst.*, vol. 36, no. 3, pp. 965–973, Jul. 2000.

[40] M. Cespedes, L. Xing, and J. Sun, "Constant-power load system stabilization by passive damping," *IEEE Trans. Power Electron.*, vol. 26, no. 7, pp. 1832–1836, Jul. 2011.

[41] A. A. A. Radwan and Y. A.-R. I. Mohamed, "Linear active stabilization of converter-dominated DC microgrids," *IEEE Trans. Smart Grid*, vol. 3, no. 1, pp. 203–216, Mar. 2012.

[42] P. Liutanakul, A.-B. Awan, S. Pierfederici, B. Nahid-Mobarakeh, and F. Meibody-Tabar, "Linear stabilization of a DC bus supplying a constant power load: A general design approach," *IEEE Trans. Power Electron.*, vol. 25, no. 2, pp. 475–488, Feb. 2010.

[43] A. Kwasinski and C. N. Onwuchekwa, "Dynamic behavior and stabilization of DC microgrids with instantaneous constant-power loads," *IEEE Trans. Power Electron.*, vol. 26, no. 3, pp. 822–834, Mar. 2011.

[44] P. Magne, B. Nahid-Mobarakeh, and S. Pierfederici, "General active global stabilization of multiloads DC-power networks," *IEEE Trans. Power Electron.*, vol. 27, no. 4, pp. 1788–1798, Apr. 2012.

[45] D. Linden and T. B. Reddy, *Handbook of Batteries*. New York, NY, USA: McGraw-Hill, 2002.

[46] L. Guo, J. Y. Hung, and R. M. Nelms, "Evaluation of DSP-based PID and fuzzy controllers for DC-DC converters," *IEEE Trans. Ind. Electron.*, vol. 56, no. 6, pp. 2237–2248, Jun. 2009.

[47] N. L. Diaz, T. Dragicevic, J. C. Vasquez, and J. M. Guerrero, "Intelligent distributed generation and storage units for DC microgrids—A new concept on cooperative control without communications beyond droop control," *IEEE Trans. Smart Grid*, vol. 5, no. 5, pp. 2476–2485, Sep. 2014.

[48] C. N. Onwuchekwa and A. Kwasinski, "Analysis of boundary control for buck converters with instantaneous constant-power loads," *IEEE Trans. Power Electron.*, vol. 25, no. 8, pp. 2018–2032, Aug. 2010.

[49] S. William Levine, *The Control Handbook*. Boca Raton, FL, USA: CRC Press, 2010.

[50] M. Lee, D. Chen, K. Huang, C.-W. Liu, and B. Tai, "Modeling and design for a novel adaptive voltage positioning (AVP) scheme for multiphase VRMs," *IEEE Trans. Power Electron.*, vol. 23, no. 4, pp. 1733–1742, Jul. 2008.

[51] C.-J. Chen, D. Chen, C.-S. Huang, M. Lee, and E. K.-L. Tseng, "Modeling and design considerations of a novel high-gain peak current control scheme to achieve adaptive voltage positioning (AVP) for DC power converters," *IEEE Trans. Power Electron.*, vol. 24, no. 12, pp. 2942–2950, Dec. 2009.

[52] H.-H. Huang, C.-Y. Hsieh, J.-Y. Liao, and K.-H. Chen, "Adaptive droop resistance technique for adaptive voltage positioning in boost DC–DC converters," *IEEE Trans. Power Electron.*, vol. 26, no. 7, pp. 1920–1932, Jul. 2011.

[53] X. Lu, J. M. Guerrero, K. Sun, and J. C. Vasquez, "An improved droop control method for DC microgrids based on low bandwidth communication with DC bus voltage restoration and enhanced current sharing accuracy," *IEEE Trans. Power Electron.*, vol. 29, no. 4, pp. 1800–1812, Apr. 2014.

[54] Y. Gu, X. Xiang, W. Li, and X. He, "Mode-adaptive decentralized control for renewable DC microgrid with enhanced reliability and flexibility," *IEEE Trans. Power Electron.*, vol. 29, no. 9, pp. 5072–5080, Sep. 2014.

[55] D. Boroyevich, I. Cvetkovic, D. Dong, R. Burgos, F. Wang, and F. Lee, "Future electronic power distribution systems: A contemplative view," in *Proc. Int. Conf. Optim. Electr. Electron. Equip.*, 2010, pp. 1369–1380.

[56] K. Strunz, E. Abbasi, and D. N. Huu, "DC microgrid for wind and solar power integration," *IEEE J. Emerg. Sel. Topics Power Electron.*, vol. 2, no. 1, pp. 115–126, Mar. 2014.

[57] C. Gavriluta, I. J. Candela, C. Citro, J. Rocabert, and P. Rodriguez, "Decentralized primary control of MTDC networks with energy storage and distributed generation," *IEEE Trans. Ind. Appl.*, vol. 50, no. 6, pp. 4122–4131, Nov./Dec. 2014.

[58] Y. Gu, W. Li, and X. He, "Frequency-coordinating virtual impedance for autonomous power management of DC microgrid," *IEEE Trans. Power Electron.*, vol. 30, no. 4, pp. 2328–2337, Apr. 2015.

[59] T. Dragicevic, S. Sucic, J. C. Vasquez, and J. M. Guerrero, "Flywheel-based distributed bus signalling strategy for the public fast charging station," *IEEE Trans. Smart Grid*, vol. 5, no. 6, pp. 2825–2835, Nov. 2014.

[60] N. Hur, J. Jung, and K. Nam, "A fast dynamic DC-link power-balancing scheme for a PWM converter-inverter system," *IEEE Trans. Ind. Electron.*, vol. 48, no. 4, pp. 794–803, Aug. 2001.

[61] A. Gkountaras, S. Dieckerhoff, and T. Sezi, "Performance analysis of hybrid microgrids applying SoC-adaptive droop control," in *Proc. 16th Eur. Conf. Power Electron. Appl.*, 2014, pp. 1–10.

[62] E. Liegmann and R. Majumder, "An efficient method of multiple storage control in microgrids," *IEEE Trans. Power Syst.*, vol. 30, no. 6, pp. 3437–3444, Nov. 2015.

[63] H. C. Ferreira, L. Lampe, J. Newbury, and T. G. Swart, *Power Line Communications: Theory and Applications for Narrowband and Broadband Communications Over Power Lines*. New York, NY, USA: Wiley, 2010.

[64] REbus DC Microgrid. (2015). [Online]. Available: http://rebuspower.com/technical.shtml

[65] T. Dragicevic, J. M. Guerrero, and J. C. Vasquez, "A distributed control strategy for coordination of an autonomous LVDC microgrid based on power-line signaling," *IEEE Trans. Ind. Electron.*, vol. 61, no. 7, pp. 3313–3326, Jul. 2014.

[66] W. Stefanutti, S. Saggini, P. Mattavelli, and M. Ghioni, "Power line communication in digitally controlled DC-DC converters using switching frequency modulation," *IEEE Trans. Ind. Electron.*, vol. 55, no. 4, pp. 1509–1518, Apr. 2008.

[67] F. Valenciaga and P. F. Puleston, "Supervisor control for a stand-alone hybrid generation system using wind and photovoltaic energy," *IEEE Trans. Energy Convers.*, vol. 20, no. 2, pp. 398–405, Jun. 2005.

[68] F. Valenciaga and P. F. Puleston, "High-order sliding control for a wind energy conversion system based on a permanent magnet synchronous generator," *IEEE Trans. Energy Convers.*, vol. 23, no. 3, pp. 860–867, Sep. 2008.

[69] G. Byeon, T. Yoon, S. Oh, and G. Jang, "Energy management strategy of the DC distribution system in buildings using the EV service model," *IEEE Trans. Power Electron.*, vol. 28, no. 4, pp. 1544–1554, Apr. 2013.

[70] L. Che and M. Shahidehpour, "DC microgrids: Economic operation and enhancement of resilience by hierarchical control," *IEEE Trans. Smart Grid*, vol. 5, no. 5, pp. 2517–2526, Sep. 2014.

[71] C. Jin, P. Wang, J. Xiao, Y. Tang, and F. H. Choo, "Implementation of hierarchical control in DC microgrids," *IEEE Trans. Ind. Electron.*, vol. 61, no. 8, pp. 4032–4042, Aug. 2014.

[72] X. Lu, J. M. Guerrero, K. Sun, J. C. Vasquez, R. Teodorescu, and L. Huang, "Hierarchical control of parallel AC-DC converter interfaces for hybrid microgrids," *IEEE Trans. Smart Grid*, vol. 5, no. 2, pp. 683–692, Mar. 2014.

[73] B. Wang, M. Sechilariu, and F. Locment, "Intelligent DC microgrid with smart grid communications: Control strategy consideration and design," *IEEE Trans. Smart Grid*, vol. 3, no. 4, pp. 2148–2156, Dec. 2012.

[74] Q. Shafiee, T. Dragicevic, J. C. Vasquez, and J. M. Guerrero, "Hierarchical control for multiple DC-microgrids clusters," *IEEE Trans. Energy Convers.*, vol. 29, no. 4, pp. 922–933, Dec. 2014.

[75] R. Olfati-Saber, J. A. Fax, and R. M. Murray, "Consensus and cooperation in networked multi-agent systems," *Proc. IEEE*, vol. 95, no. 1, pp. 215–233, Jan. 2007.

[76] R. Olfati-Saber and R. M. Murray, "Consensus problems in networks of agents with switching topology and time-delays," *IEEE Trans. Autom. Control*, vol. 49, no. 9, pp. 1520–1533, Sep. 2004.

[77] Z. Meng, W. Ren, Y. Cao, and Z. You, "Leaderless and leader-following consensus with communication and input delays under a directed network topology," *IEEE Trans. Syst. Man, Cybern. B, Cybern.*, vol. 41, no. 1, pp. 75–88, Feb. 2011.

[78] X. Lin and S. Boyd, "Fast linear iterations for distributed averaging," in *Proc. IEEE 42nd Int. Conf. Decision Control*, 2003, vol. 5, pp. 4997–5002.

[79] F. L. Lewis, Z. Qu, A. Davoudi, and A. Bidram, "Secondary control of microgrids based on distributed cooperative control of multi-agent systems," *IET Gener. Transmiss. Distrib.*, vol. 7, no. 8, pp. 822–831, 2013.

[80] H. Behjati, A. Davoudi, and F. Lewis, "Modular DC-DC converters on graphs: Cooperative control," *IEEE Trans. Power Electron.*, vol. 29, no. 12, pp. 6725–6741, Dec. 2014.

[81] S. Abhinav, G. Binetti, A. Davoudi, and F. L. Lewis, "Toward consensus-based balancing of smart batteries," in *Proc. IEEE 29th Annu. Appl. Power Electron. Conf. Expo.*, 2014, pp. 2867–2873.

[82] R. W. Erickson and D. Maksimovic, *Fundamentals of Power Electronics*. New York, NY, USA: Springer, 2001.

[83] J. Liu, X. Feng, F. C. Lee, and D. Borojevich, "Stability margin monitoring for DC distributed power systems via perturbation approaches," *IEEE Trans. Power Electron.*, vol. 18, no. 6, pp. 1254–1261, Nov. 2003.

[84] M. Shirazi, R. Zane, and D. Maksimovic, "An autotuning digital controller for DC-DC power converters based on online frequency-response measurement," *IEEE Trans. Power Electron.*, vol. 24, no. 11, pp. 2578–2588, Nov. 2009.

[85] J. A. Abu Qahouq and V. Arikatla, "Online closed-loop autotuning digital controller for switching power converters," *IEEE Trans. Ind. Electron.*, vol. 60, no. 5, pp. 1747–1758, May 2013.

[86] J. Morroni, R. Zane, and D. Maksimovic, "Design and implementation of an adaptive tuning system based on desired phase margin for digitally controlled DC-DC converters," *IEEE Trans. Power Electron.*, vol. 24, no. 2, pp. 559–564, Feb. 2009.

[87] A. Barkley and E. Santi, "Improved online identification of a D-DC converter and its control loop gain using cross-correlation methods," *IEEE Trans. Power Electron.*, vol. 24, no. 8, pp. 2021–2031, Aug. 2009.

[88] J. Morroni, R. Zane, and D. Maksimovic, "An online stability margin monitor for digitally controlled switched-mode power supplies," *IEEE Trans. Power Electron.*, vol. 24, no. 11, pp. 2639–2648, Nov. 2009.

[89] P. Kundur, N. J. Balu, and M. G. Lauby, *Power System Stability and Control*. New York, NY, USA: McGraw-Hill, 1994.

[90] A. Riccobono and E. Santi, "Comprehensive review of stability criteria for DC power distribution systems," *IEEE Trans. Ind. Appl.*, vol. 50, no. 5, pp. 3525–3535, Sep./Oct. 2014.

[91] M. K. Zamierczuk, R. C. Cravens, and A. Reatti, "Closed-loop input impedance of PWM buck-derived DC-DC converters," in *Proc. IEEE Int. Symp. Circuits Syst.*, 1994, vol. 6, pp. 61–64.

[92] R. D. Middlebrook, "Null double injection and the extra element theorem," *IEEE Trans. Edu.*, vol. 32, no. 3, pp. 167–180, Aug. 1989.

[93] A. M. Rahimi and A. Emadi, "An analytical investigation of DC/DC power electronic converters with constant power loads in vehicular power systems," *IEEE Trans. Veh. Technol.*, vol. 58, no. 6, pp. 2689–2702, Jul. 2009.

[94] P. A. Dahono, "A control method for DC-DC converter that has an LCL output filter based on new virtual capacitor and resistor concepts," in *Proc. IEEE 35th Annu. Power Electron. Spec. Conf.*, 2004, vol. 1, pp. 36–42.
[95] X. Lu, K. Sun, J. M. Guerrero, J. C. Vasquez, L. Huang, and J. Wang, "Stability enhancement based on virtual impedance for DC microgrids with constant power loads," *IEEE Trans. Smart Grid*, to be published.
[96] X. Liu, A. J. Forsyth, and A. M. Cross, "Negative input-resistance compensator for a constant power load," *IEEE Trans. Ind. Electron.*, vol. 54, no. 6, pp. 3188–3196, Dec. 2007.
[97] A. Kwasinski and P. T. Krein, "Passivity-based control of buck converters with constant-power loads," in *Proc. IEEE Power Electron. Spec. Conf.*, 2007, pp. 259–265.
[98] J. Wang and D. Howe, "A power shaping stabilizing control strategy for DC power system with constant power loads," *IEEE Trans. Power Electron.*, vol. 23, no. 6, pp. 2982–2989, Nov. 2008.
[99] A. M. Rahimi, G. A. Williamson, and A. Emadi, "Loop-cancellation technique: A novel nonlinear feedback to overcome the destabilizing effect of constant-power loads," *IEEE Trans. Veh. Technol.*, vol. 59, no. 2, pp. 650–661, Feb. 2010.
[100] A. P. N. Tahim, D. J. Pagano, M. L. Heldwein, and E. Ponce, "Control of interconnected power electronic converters in DC distribution systems," in *Proc. Brazilian Power Electron. Conf.*, 2011, pp. 269–274.

Tomislav Dragičević (S'09–M'13) received the M.E.E. and the industrial Ph.D. degrees from the Faculty of Electrical Engineering, Zagreb, Croatia, in 2009 and 2013, respectively. His Ph.D. dissertation has been carried out in close cooperation with industry and he has received highest honours for it.

He is currently a Postdoctoral Research Associate at the Institute of Energy Technology, Aalborg University, Aalborg, Denmark. He has authored and coauthored more than 60 technical papers in his domain of interest, 18 of them are published in international journals. His research interests include overall system design of autonomous and grid-connected dc and ac microgrids, and industrial application of advanced modeling, control, and protection concepts to shipboard power systems, remote telecom stations, domestic and commercial facilities, and electric vehicle charging stations.

Dr. Dragičević is a Member of the IEEE Power Electronics and IEEE Power Systems Societies. He has served in Scientific Committee Boards in several IEEE conferences and has been invited for guest lectures and tutorials in a number of universities and companies around the world.

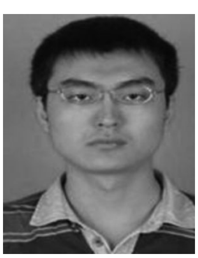

Xiaonan Lu (S'11–M'14) was born in Tianjin, China, 1985. He received the B.E. and Ph.D. degrees in electrical engineering from Tsinghua University, Beijing, China, in 2008 and 2013, respectively. From September 2010 to August 2011, he was a Guest Ph.D. Student with the Department of Energy Technology, Aalborg University, Aalborg, Denmark.

From October 2013 to December 2014, he was a Postdoctoral Researcher with the Department of Electrical Engineering and Computer Science, University of Tennessee, Knoxville, USA. In January 2015, he joined the Energy Systems Division, Argonne National Laboratory, Lemont, IL, USA, where he is currently a postdoctoral Researcher. His research interests include modeling and control of power electronic converters in renewable energy systems and microgrids, hardware-in-the-loop real-time test, multilevel converters, matrix converters, etc.

Dr. Lu received the Outstanding Reviewer Award for the IEEE TRANSACTIONS ON POWER ELECTRONICS in 2014. He is a Member of the PELS, the IAS, and the PES Society.

Juan C. Vasquez (M'12–SM'14) received the B.S. degree in electronics engineering from the Autonomous University of Manizales, Manizales, Colombia, in 2004, and the Ph.D. degree in automatic control, robotics, and computer vision from the Technical University of Catalonia, Barcelona, Spain, in 2009.

From February 2015 to April 2015, he was a Visiting Scholar with the Center of Power Electronics Systems, Virginia Tech.

In 2011, he was an Assistant Professor in microgrids and he is currently an Associate Professor at the Department of Energy Technology, Aalborg University, Aalborg, Denmark. He is coresponsible of the Research Program in Microgrids. His current research interests include operation, power management, hierarchical control, optimization and power quality applied to distributed generation, and ac/dc microgrids.

Dr. Vasquez is currently a Member of the IEC System Evaluation Group SEG4 on LVDC Distribution and Safety for use in Developed and Developing Economies and the Renewable Energy Systems Technical Committee TC-RES in the IEEE Industrial Electronics Society.

Josep M. Guerrero (S'01–M'04–SM'08–F'15) received the B.S. degree in telecommunications engineering, the M.S. degree in electronics engineering, and the Ph.D. degree in power electronics from the Technical University of Catalonia, Barcelona, Spain, in 1997, 2000, and 2003, respectively.

Since 2011, he has been a Full Professor at the Department of Energy Technology, Aalborg University, Aalborg, Denmark, where he is responsible for the Microgrid Research Program. Since 2012, he has been a Guest Professor at the Chinese Academy of Science, Beijing, China, and the Nanjing University of Aeronautics and Astronautics, Jiangsu, China; since 2014, he has been a Chair Professor at Shandong University, Jinan, China; and since 2015, he has been a Distinguished Guest Professor at Hunan University, Changsha, China. His research interests include different microgrid aspects, including power electronics, distributed energy-storage systems, hierarchical and cooperative control, energy management systems, and optimization of microgrids and islanded minigrids.

Prof. Guerrero is an Associate Editor for the IEEE TRANSACTIONS ON POWER ELECTRONICS, the IEEE TRANSACTIONS ON INDUSTRIAL ELECTRONICS, and the IEEE INDUSTRIAL ELECTRONICS MAGAZINE, and an Editor for the IEEE TRANSACTIONS ON SMART GRID and the IEEE TRANSACTIONS ON ENERGY CONVERSION. He was the Chair of the Renewable Energy Systems Technical Committee of the IEEE Industrial Electronics Society. In 2014, he received the Highly Cited Researcher Award by Thomson Reuters.